EVALUATING THE REDUCTION IN SNUBBING WITH SOFT-RECOVERY DEVICES AND THE AFFECT OF RESISTOR INDUCTANCE

F.V.P. Robinson,
University of Bath,
Bath,
England, U.K.

B. W. Williams,
Heriot-Watt University,
Edinburgh,
Scotland, U.K.

ABSTRACT

Fast current-fall is normally a desired characteristic for power devices because turn-off crossover time and switching power-loss are minimised; but with power-rectifiers, an abrupt termination to reverse-recovery is considered undesirable because high-amplitude voltage-overshoot and oscillations are produced by unavoidable circuit inductance resonating with device junction-capacitance; and the application of RC-snubber circuits, using practical resistors with significant parasitic inductance, is complicated. This has led device manufacturers to examine and modify diode geometry and processing to control current-fall, as well as, total recovered-charge during reverse-recovery. However, the affect of soft current-fall on RC-snubber performance seems not to have been previously examined over a range of fall types and snubber conditions. This paper examines how current-fall shape affects RC-snubber performance, to determine if smaller snubbers can be used which remain tolerant to varying current-fall shape and duration and give lower power-loss.

INTRODUCTION

The established design procedure for RC-snubbers, controlling diode reverse-recovery transients [13], assumes that the termination of reverse current approximates to an instantaneous current fall, and that peak reverse current, I_{RM}, is simultaneously commutated from the diode to an RC-snubber. While this is valid, where circuit inductance controlling reverse-recovery is high enough to necessitate a snubber with a natural period of voltage response much greater than the diode-current fall-time, it is less adequate for soft-recovery diodes or high-frequency power convertors using low-inductance hardware-practice, where the natural period of snubber response approaches diode-current fall-time; because a significant fraction of the energy trapped in stray or circuit inductance, normally absorbed by the snubber ($1/2\ L_S I_{RM}^2$) is dissipated in the diode. This seems to imply that less capacitance than predicted by the 'abrupt' design procedure can be used with soft-recovery diodes, for the same level of overshoot, providing the diodes can dissipate the resulting higher peak and average power-loss. It will be shown that this is only true for a limited range of circuit conditions; and, where these are met and reduced snubbers are used, an important consideration in their application is shown to be voltage-response sensitivity to current-fall variation. Consistent current-fall behaviour cannot be relied upon, because fall shape and duration are determined by device geometry, processing, and operating conditions [1-7], and are further affected by diode/snubber interaction because diode reverse-voltage-rise waveform affects current fall [8,9].

The purpose of this paper is to establish if it is worthwhile to assume that current-fall is other than abrupt in RC-snubber design. The data generated to do this, also, serves to illustrate the danger of empirically sizing RC-snubbers, without testing under different operating condition extremes, or without performing follow-up worst-case analysis.

RC-SNUBBER PERFORMANCE WITH COMPONENT IMPERFECTIONS

The RC-snubber optimization procedure of [13] has more to recommend it that other methods. It uses the fact that for any set of E_{DC}, L_S and I_{RM} values (Fig.1) an optimal pair of R and C values exist which minimizes snubber energy-loss for any overshoot level. Optimal R and C values are specified by the graphs of Figure 2. Initial current factor χ, and damping factor ζ, (Eq.1 and 2) specify, respectively, C and R

$$\chi = I_{RM}/E_{DC}\sqrt{L_S/C} \qquad (1)$$

$$\zeta = R/2\sqrt{C/L_S} \qquad (2)$$

Over a limited range of normalised overshoot, V_{OSN}, the relationship between V_{OSN} and χ can be approximated as in Equation 3.

$$\chi \approx 1.51\ V_{OSN} + 0.24 \quad , \text{ for } 20\% < V_{OSN} < 100\% \qquad (3)$$

Where dv/dt value is of concern, e.g. thyristor snubbing, an average dv/dt graph can be added to Figure 2, or the optimisation criteria can be changed to setting dv/dt-V_{OSN} product with minimal C [13], rather than V_{OSN}. χ (Fig. 2) is normally considered to be varied by changing C (Eq.1) because other terms are set by the design. If χ is changed by I_{RM} variation alone, for fixed snubbers, overshoot varies as in Figure 3. Above the peak design I_{RM}, peak overshoot increases more rapidly; in proportion to current (Eq.5) in the linear regions. Normalised initial snubber voltage,

$$I_{RM}\ R\ /\ E_{DC} = 2\ \zeta\ \chi \qquad (5)$$

Before the linear regions, not necessarily at or below the design I_{RM}, the initial voltage-rise is also set by Equation 5, but its voltage is less than the peak value. The initial voltage-rise exceeds peak overshoot when the curves become linear. Peak overshoot is then accurately predictable (Eq.5).

In practice, the initial overshoot will depend on reverse-current fall-time, snubber-resistor parasitic-inductance and effective diode capacitance. Because resistor inductance is relatively high (Fig. 5), significant additional overshoot may be superimposed on the ohmic voltage drop, especially with very fast current fall (Fig. 4,5 and 6).

Practical 30 A, 1000 V and 1200 V epitaxial diodes, intended for high-frequency power conversion (≥10kHz) were measured to have current fall di/dt in the range 500-2000A/µs for recovery di/dt between 100 and 1000 A/µs and would give 500 V to 2000 V overshoot per µH of snubber resistor inductance. Recovery waveform measurements were made using a simple chopper circuit (Fig.1) with a capacitor-based voltage clamp

90/CH 2935-5/90/0000-1686$01.00©1990 IEEE

to limit peak diode-voltage, and significant overshoot was even produced on the parasitic clamp inductance (100nH), which subsequently resonates at 40MHz with diode junction-capacitance (Fig.6a).

The waveforms (Fig.6) show attainable values of current fall di/dt, after the controlled recovery di/dt period, albeit under artificial operating conditions. Because a voltage clamp is used, reverse current can only fall when reverse diode-voltage exceeds E_{DC}. A faster voltage-rise is obtained which generally accelerates the final stages of reverse recovery and gives snappier current-fall. This effect is observable with RC-snubbers. As diode dv/dt is increased, by increasing snubber resistance, current-fall shape can change from being approximately exponential to linear [8].

It is evident, therefore, that diodes of similar ratings cannot be relied upon to give consistent reverse-recovery characteristics. However, diodes with soft-recovery characteristics will generally be more forgiving of RC-snubber inductance and facilitate the control of overshoot and ringing.

RC-SNUBBERS WITH NON-ABRUPT CURRENT FALL

To represent different current-fall shapes observed experimentally and in references [1-8], five simple functions are defined (Appendix A), which are plotted in Figure 7. Normalized current fall-time, τ_N, (time-constant for exponential) and a modified initial current factor, λ, are required to take into account fall-time variability, and are specified by Equations 6 and 7, as in [12].

$$\tau_N = \omega_o \tau = \tau / \sqrt{L_S C} \quad (6)$$

$$\lambda = I_{RM} L_S / E_{DC} \tau \quad (7)$$

$$\chi = \lambda \tau_N \quad (8)$$

The peak voltage-overshoot for three snubbers, designed to give 20, 60 and 100% overshoot with abrupt current-fall, is calculated for each of the current-fall shapes assuming no other operating conditions change, for a range of normalized fall time τ_N, and is plotted in Figure 8. χ for the abrupt snubbers is obtained from Figure 2. The λ axis represents a range of τ_N, since χ is held constant for each overshoot level, and Equation 8 is upheld for otherwise constant operating conditions. Peak overshoot is obtained by numerical solution of circuit state equations (Appendix B).

The peak voltage overshoot curves are as expected at the λ value extremes (Fig.8). At high λ, τ is small relative to $\sqrt{L_S C}$, i.e. L_S is high and C is higher to control greater trapped-energy. Hence, current-fall appears abrupt relative to response natural-period (Fig.9). These waveforms are used here, simply to illustrate relative abruptness for exponential current-fall. They, actually, apply to the graphs of Figure 10. At low λ (Fig.9d), τ significantly overlaps the snubber response period and most of the trapped energy at the peak of diode recovery ($1/2 L_S I_{RM}^2$) is dissipated in the diode. The effect is similar to operating the snubber at a lower current. Smaller capacity snubbers are required to raise overshoot to the design level. Peak overshoot is higher for mid-range λ values (Fig.8) because, during the peak of diode recovery, L_S experiences a greater positive voltage/time integral, which increases the current and energy trapped in L_S (Fig.9c). For this reason, current-fall shapes closer to an extended flat period of I_{RM}, i.e. square and haversine (Fig.7), produce a greater increase in overshoot with 'abrupt' snubbers (Fig.8) than fall shapes which rapidly fall away from I_{RM}, i.e. root and linear (N.B. initial voltage overshoot due to resistor inductance is not considered here). Exponential current-fall is an exception because its extended fall period results in more trapped energy being diverted from the snubber when the diode voltage exceeds E_{DC}. The 'square' fall type gives a greater fall in overshoot when the voltage on L_S changes from positive to negative during most of the current fall, at low λ values, because greater trapped energy is put into a 'square' fall than 'root' fall diode, i.e. it takes significantly more current and thus energy than the snubber during the period of overshoot and current-fall overlap.

Current-fall variation has a greater affect on the overshoot of light (100%) 'abrupt' snubbers because the energy controlled by the snubber (Eq.4) is lower and more easily disturbed by extra energy added to L_S, or diverted from the snubber to the diode, as previously described.

Variation in the overshoot obtained with 'abrupt' snubbers on non-abrupt current-fall devices will be of little consequence in most cases, especially with approximately exponential current fall, other than to introduce greater discrepancy between predicted and experimental overshoot. The danger of despairing of being able to design snubbers analytically and employing values virtually arrived at by trial and error is evident from Figure 8. Snubbers empirically optimised at λ between 0.1 and 10.0 have the potential to give significantly greater overshoot if current-fall time or shape variation occurs. This is quantified in the next section by optimizing RC-snubbers for each of the current-fall shapes and observing the variation in overshoot, produced by subjecting these to fall type and duration variation.

OPTIMIZING RC-SNUBBERS WITH NON-ABRUPT CURRENT FALL

Ray [12] produced basic design graphs for optimal RC-snubbers, for diodes with approximately exponential current fall, in a procedure which parallels McMurray's [13]. The graphs, similar to Figure 10, specify minimum snubber capacitance and corresponding resistance to set a required level of overshoot for specified I_{RM}, E_{DC}, L_s and τ, i.e. λ (Eq.7). This data is easier to use and can cover wider ranges of λ and τ_N values when sorted for specific overshoot levels as in Figure 11. Similarly, optimal RC-snubbers for other current-fall types can be derived. Graphs for 'linear' snubbers are given in Figure 12 and for all current fall types in Figure 13 for three levels of overshoot. Graphs are terminated when excessive computational difficulty is experienced searching for minimum values on very slowly changing curves or in regions of several minima.

Since snubber capacitance for 'abrupt' snubbers is defined by χ (Eq.1), which is definable in terms of soft current-fall parameters, τ_N and τ (Eq.8), the difference in snubber capacitance required by soft current-fall snubbers is represented by the separation of the graphs in Figure 13 from the lines of constant χ. For τ_N below constant χ lines more capacitance is

required than for the equivalent 'abrupt' snubber. In the λ ranges shown, only 'exponential' snubbers are seen to require less capacitance, but graphs for other fall types should follow the 'exponential' graph at lower λ. A more complete examination of 'exponential' snubbers is conducted because an exponential current fall approximation is often used to model soft-recovery diodes.

SENSITIVITY OF NON-ABRUPT SNUBBERS TO CURRENT FALL VARIATION

Optimal 60% RC-snubbers for each current-fall type (Fig.13) are subjected to other current-fall types, including abrupt fall, and the resulting peak overshoot levels are plotted in Figure 14. Clearly snubbers optimized for exponential fall are least tolerant of other falls, especially 'abrupt' and 'root' types, which have regions of higher fall di/dt than the others. Response sensitivity to fall shape variation is generally determined by capacitor value, which is determined from τ_N (Eq.6) or rather the τ_N-λ product. Since higher τ_N implies smaller capacitance, at λ=1, the 'exponential' snubber is least tolerant and the 'square' snubber the most tolerant of fall type variation. More so, in fact, than the 'abrupt' snubber represented by the constant χ line.

Likewise, by varying current-fall time or time-constant by factors between 0 and 5 for optimal 60% snubbers in Figure 13, response sensitivity to fall duration can be assessed by plotting the resulting peak overshoot (Fig.15). Here, also, exponential snubbers remain the least tolerant to change, but the ordering of other fall types reverses, and 'square' and 'root' snubbers are seen to be, respectively, the least and more tolerant to fall duration variation. The reason is similar to that previously given to explain the rise in peak overshoot level above the 'abrupt' level in Figure 8. 'Square' and 'haversine' current profiles result in greater increase in trapped energy in L_S, more of which is put into the snubber than dissipated in the diode. The effect becomes more pronounced with extended current-fall time.

Response sensitivity variation to both current-fall type and duration variation improves with heavier snubbing (Fig.16 and 17) as found with 'abrupt' snubbers (Fig.8). In Figure 16 three linear snubber designs are subjected to varying fall type and in Figure 17 three exponential snubber designs are subjected to varying duration.

To summarize this section, it is seen in Figure 13 that optimal 'exponential' snubbers under certain conditions require less capacitance than 'abrupt' snubbers e.g. λ<0.75 for 60% exponential snubbers. However, response sensitivity to variation in current-fall shape and duration increases dramatically, especially if the current-fall has regions of high di/dt as with 'abrupt' or 'root' falls (Fig.14) or the fall duration reduces (Fig.15). With either type of fall variation, voltage response change will be greater with lighter snubbing, chosen to set higher nominal overshoot (Fig.16 and 17). Where 'abrupt' snubbers are used with soft-recovery diodes, an appreciation of the degree of error caused by non-abrupt current fall is obtainable from the graphs in Figure 8, using diode snappiness factor, S which is related to λ (Eq.9a).

$$\lambda = I_{RM}L_S/E_{DC}\tau = [I_{RM}/\ di/dt]/\tau = k\ S \qquad (9a)$$

The JEDEC snappiness factor, S, must be multiplied by a fall-type dependant factor to compensate for the different fall-time definitions used for λ and S.

ENERGY-LOSS ASSOCIATED WITH NON-ABRUPT SNUBBERS

The energy-loss associated with 'exponential' snubbers has previously been presented in a similar way to Figure 18 for the circuit conditions given in Figure 10. Energy-loss is normalised to a base of energy dissipated in the diode with no RC-snubber (Eq.9b).

$$W_B = E_{DC}I_{RM}\tau + 1/2\ L_S\ I_{RM}^2 = E_{DC}I_{RM}\tau\ (1 + \lambda/2) \qquad (9b)$$

To alleviate difficulty in gaining insight into energy-loss variation from Figure 19, and distribution between snubber and diode with changing current fall-time, it is better to plot energy-loss for specific overshoot levels (Fig.20). Also, to enable direct comparison of energy-loss graphs for different current-fall types and durations, energy-loss has to be normalised to a base of initial trapped energy, $1/2L_SI_{RM}^2$, as in Figure 21 for exponential current-fall.

At high λ (>10), τ is small relative to $\sqrt{L_SC}$ (Fig.9) and the total energy-loss curve is asymptotic to the normalized loss of an 'abrupt' RC-snubber during the voltage-rise (Eq.10), e.g. for 40% overshoot, χ=0.85 from Figure.2 and W_{TN}=2.4 (see 40% curve in Fig.21).

$$W_{TN} = W_T\ /\ 1/2\ L_SI_{RM}^2 = (\ 1 + 1/\chi^2) \qquad (10)$$

The variation in total energy-loss above the 'abrupt' snubber asymptote, results from the increased snubber capacitance required at lower λ, since

$$C_2 = (\ \tau_{N1}/\ \tau_{N2}\ )^2\ C_1 \qquad (11)$$

and greater v-i crossover loss due to the lengthening exponential current-fall. Although RC-snubber loss reduces at low λ, the increase in diode crossover loss (Fig.9c) with decreasing λ prevents the net energy-loss of an optimal 'exponential' snubber and soft-recovery diode, operating at constant current, ever being more efficient than an abrupt diode and snubber.

Where RC-snubber loss is small total energy-loss approximates to diode loss (Eq.12)

$$W_D = E_{DC}I_{RM}\tau + 1/2\ L_SI_{RM}^2 = (2/\lambda + 1)\ 1/2\ L_SI_{RM}^2 \qquad (12)$$

Normalising this to abrupt snubber loss, W_T, (Eq.10);

$$W_{DN} = (\ 2/\lambda + 1\ )\ /\ (\ 1 + 1/\chi^2\ ) \qquad (13)$$

Equation 13, in conjunction with Figure 21, confirms that, for very small λ, total loss will never fall below that of the abrupt diode and snubber. Absolute diode and RC-snubber loss is given by Equation 12, and confirms energy-loss values for low λ [Fig.21].

Energy-loss curves for current-fall types other than the exponential, also, lie further above the 'abrupt' snubber energy-loss level as λ is reduced (Fig.22). Diode energy loss is significantly lower because of the reduced voltage rise time as seen in Figure 13a.

So far, constant forward-current diode operation has been assumed, and total energy-loss is higher for soft-recovery diodes with reduced snubbers than abrupt diodes and snubbers. However, where power-

device forward current is modulated, RC-snubbers may be under utilised because I_{RM} varies with I_F, particularly if recovery di/dt is high, and may be less than the design value, $I_{RM(max)}$, for significant periods. Total snubber energy-loss for turn-on and off is then given by equation 14.

$$W_S = L_S I_{RM}^2 / 2 + (2/\chi^2) \; L_S I_{RM(max)}^2 / 2 \qquad (14)$$

The I_{RM} term is modulated by I_F variation, whereas the $I_{RM(max)}$ term represents a high constant energy-loss term. Also, using snubbers on series-connected power-devices in bridge-legs, doubles the high constant energy term of Equation 14, because two snubbers are continually active which are not mutually assisting during power-device reverse-recovery. To determine if a net energy-loss benefit results with reduced snubbing, average diode and snubber energy-loss must be considered.

The potential for energy-loss reduction is greatest at high overshoot levels. The graphs in Figure 13, for exponential snubbers giving high overshoot, crossover the 'abrupt' snubber constant χ lines at higher λ values, and there is an increased likelihood that the design λ lies below the intersection and requires less capacitance than the equivalent 'abrupt' snubber. For example, for a λ value of 1.14, the corresponding abrupt and exponential τ_N values for 100% snubbers are 1.5 and 3.00, respectively. Equation 11 is used to show that the optimal 'exponential' snubber uses a quarter of the capacitance of the optimal 'abrupt' snubber, under these conditions. With higher overshoot or lower λ, i.e. higher current-fall time-constant, an even greater reduction is possible. In contrast, at λ=1.14 both 10% and 60% optimal 'exponential' snubbers require about 6 and 1.5 times the capacitance of the abrupt designs.

Despite the factor of four reduction in the 100%-snubber capacitance, Figure 21 shows that the normalized total energy-loss for the optimal 'exponential' snubber and soft-recovery diode is 2.84, giving 68% higher turn-off loss than an optimal abrupt snubber diode combination, at 1.69, assuming fixed current operation in both cases. For an appreciation of the magnitude of reduction in average energy-loss sinusoidal diode current modulation is assumed to give sinusoidal I_{RM} modulation. Exponential snubber and soft-recovery diode energy-loss for a complete switching cycle is given by Equation 15.

$$W_E = [E_{DC} I_{RM} \tau + 1 + 2 / \chi^2] \; 1/2 \; L_S I_{RM}^2 \qquad (15a)$$

$$W_E = [2 / \lambda + 1 + 2 / (\lambda \tau_N)^2] \; 1/2 L_S I_{RM}^2 \qquad (15b)$$

The accuracy of Equation 15 can be confirmed using Figure 13 and 21, bearing in mind that snubber capacitor discharge energy is included in Equation 15 but not in Figure 21. For sinusoidal current modulation Equation 16 gives normalized average energy-loss per switching cycle (Appendix C).

$$\bar{W}_{EN} = [1/2\lambda + 1/4 + (C_2/C_1) \; 2/\chi^2)] \qquad (16)$$

Using previous data for 100% snubber design at λ=1.14, the normalized average loss for 'abrupt' and 'exponential, snubbers are 0.95 and 0.86, respectively, from Equation 16 and 17.

$$\bar{W}_{AN} \approx [1/4 + 2/\chi^2] \qquad (17)$$

The order of magnitude of average switching loss is comparable. However, with practical diodes I_{RM} varies more slowly than assumed, increasing the first two and first terms in Equation 16 and 17, respectively. For the extreme case, where I_{RM} is constant during diode I_F modulation $\bar{W}_{EN}$ is twice $\bar{W}_{AN}$, (3.45 and 1.7 respectively). Therefore, in practice, $\bar{W}_{EN}$ is more likely to exceed $\bar{W}_{AN}$, and despite the significant reduction in snubber capacitance in the optimal 'exponential' snubber, little energy-loss advantage can be expected.

CONCLUSIONS

Finely tuning RC-snubber components, to take into account non-abrupt current fall, allows reduced snubber capacitance to be used under certain operating conditions. However, voltage-responses become more sensitive to current-fall shape, diode switching-loss is increased by several orders of magnitude, and there appears to be no significant energy-loss advantage with sinusoidally modulated current. Nevertheless, the results prove useful in understanding discrepancies between predicted and practical transient response characteristics for RC-snubbers, and the dangers of empirically sizing snubbers without considering variation in reverse-recovery characteristics between devices and with operating conditions.

REFERENCES

[1] I. Somos, "Commutation and destructive oscillation in diode circuits", IEEE Trans. Comm. Elect. (part A), pp. 162-172.

[2] D.E. Houston, M.S. Adler and E.D. Wolley, "Measurement and analysis of charge distributions and their decay in fast switching power rectifiers', IEDM Technical Digest, 1977, pp. 308-312.

[3] J. Vitins, P. De Bruyre and M. Taube, "Fast high voltage power diodes with soft reverse recovery: physical and electric properties", IEEE IAS Conf. Rec., 1979, pp. 1062-1067.

[4] H.B. Assalt, L.O. Eriksson and S.J. Wu, "High power controlled soft recovery diode design and application", IAS Conf. Rec., 1979, pp. 1056-1061.

[5] G.R. Bisio et al, "Switching performance of high power fast recovery rectifiers", IEEE PESC Conf. Rec., 1981, pp. 244-251.

[6] E.D. Wolley and S.F. Beuzcqua, "High speed soft recovery epitaxial diodes for power inverter circuits", IEEE IAS Conf. Rec., 1981, pp. 797-800.

[7] C.K. Chu et al, "Design considerations on high voltage soft recovery rectifiers", IEEE IAS Conf. Rec., 1982, pp. 721-726.

[8] L.O. Erikson and W.H. Tobin, "Evaluation of high power, controlled recovery diodes", IEEE IAS Conf. Rec., 1978, pp. 1036-1043.

[9] E.I. Carroll and R.S. Chokhawala, "A snubber design tool for P-N junction reverse recovery using a more accurate simulation of the reverse recovery waveform", IEEE IAS Conf. Rec., 1989, pp. 1307-1319.

[10] P.T. Hoban, "The characterisation of snubber diodes for use with high voltage GTO thyristors", IEE PEVD, Conf. Publication 291, 1988, pp. 99-102.

[11] F.V.P. Robinson and B.W. Williams, "Systematic design of dissipative and regenerative snubbers", IEEE IAS Conf. Rec, 1989, pp. 1320- 1327.
[12] W.F. Ray, "Snubber design for diodes with soft turn-off", IEE PEVD, Conf. Publication No. 264, 1986, pp. 43-46.
[13] W. McMurray, "Optimum snubbers for power semiconductors", IEEE Trans., Vol. IA-8, No. 5, 1972, pp. 593-600.
[14] Y.Ikeda, J.Itsumi and H. Funato, "The power loss of PWM voltage fed inverter", IEEE PESC Conf.Rec.,1988, pp. 277-283.

APPENDICES

Appendix A: Normalized current fall equations

Exponential $i_{DN} = e^{-t_N/\tau_N}$

Root $i_{DN} = (1 - \sqrt{t_N/\tau_N})$

Linear $i_{DN} = (1 - t_N/\tau_N)$

Square $i_{DN} = [1 - (t_N/\tau_N)^2]$

Haversine $i_{DN} = [1 + \cos(\pi t_N/\tau_N)]/2$

Appendix B: State equations for abrupt current fall.

$$\begin{vmatrix} v'_{CN} \\ i'_{LN} \end{vmatrix} = \begin{vmatrix} 0 & \chi \\ -1/\chi & -2\zeta \end{vmatrix} \begin{vmatrix} v_{CN} \\ i_{LN} \end{vmatrix} + \begin{vmatrix} 0 \\ 1/\chi \end{vmatrix}$$

State equations for non-abrupt current fall:

$$\begin{vmatrix} v'_{CN} \\ i'_{LN} \end{vmatrix} = \begin{vmatrix} 0 & \chi \\ -1/\chi & -2\chi \end{vmatrix} \begin{vmatrix} v_{CN} \\ i_{LN} \end{vmatrix} + \begin{vmatrix} -\chi i_{DN} \\ 1/\chi + 2\zeta \end{vmatrix}$$

where i_{DN} is specified in Appendix A.

Appendix C: If switching loss can be put in the form,

$$W_{SW} = A\, i + B\, i^2$$

it can be shown that average switching loss for sinusoidal current modulation is as follows [14]:

$$\bar{W}_{SW} \approx A\, I_M/\pi + B\, I_M/4$$

If it is assumed that I_{RM} varies linearly with forward diode current, total average abrupt energy-loss is

$$\bar{W}_A \approx (1 / 4 + 2 / \chi^2)\ 1/2\ L_S I_M^2$$

With an 'exponential' snubber' and soft recovery diode total average energy-loss includes diode and snubber loss terms and for insight can be approximated as follows:

$$\bar{W}_E = [1/2\ \lambda + 1/4\ (C_2/C_1)2/\chi^2]\ 1/2\ L_S I_M^2$$

where C_2 is the 'exponential' snubber capacitor and C_1 the abrupt' snubber capacitor.

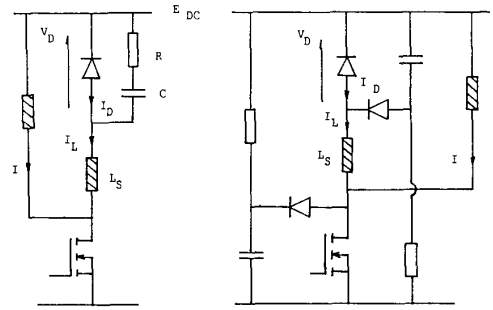

FIG.1 SINGLE-ENDED CHOPPER WITH RC-SNUBBER ON DIODE, AND CHOPPER CIRCUIT WITH CLAMPS FOR OBSERVING REVERSE-RECOVERY WAVEFORMS.

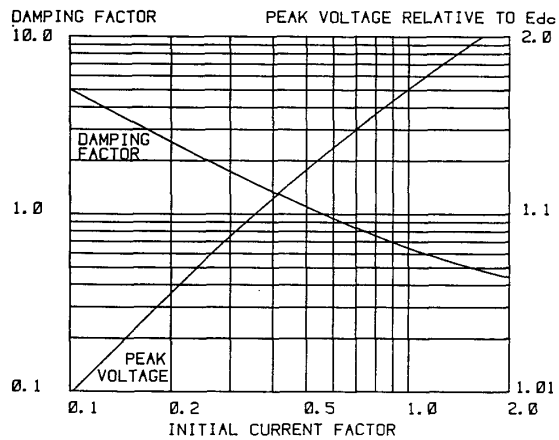

FIG.2 OVERSHOOT, V_{OSN}, AND DAMPING FACTOR, ζ, FOR OPTIMAL ABRUPT SNUBBING.

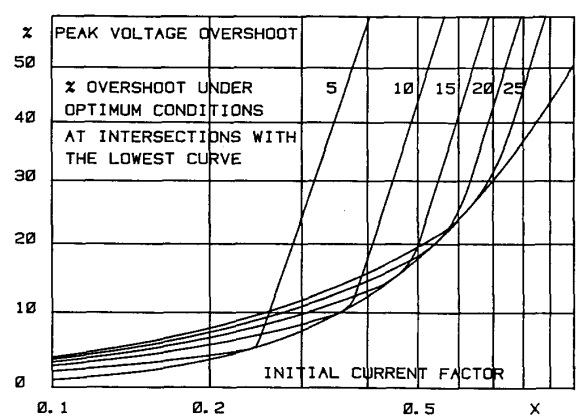

FIG.3 VARIATION IN PEAK VOLTAGE OF 15-25% SNUBBERS FOR I_{RM} EITHER SIDE OF THE DESIGN VALUE USED TO SET χ.

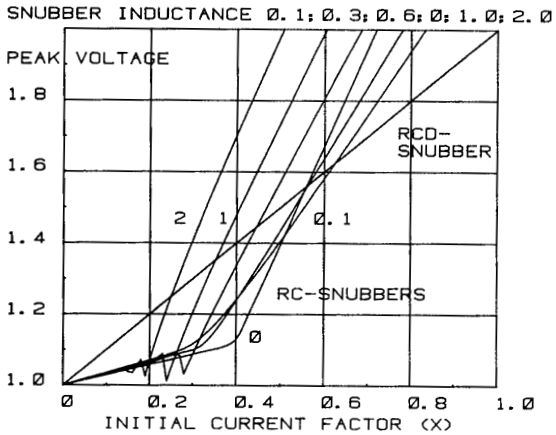

FIG.4 EFFECT OF INCREASING PARASITIC RESISTOR INDUCTANCE (NORMALISED TO Ls DEFINED IN FIGURE 1). ABRUPT DIODE-RECOVERY AND A SMALL VALUE OR DIODE JUNCTION CAPACITANCE ASSUMED. RCD-SNUBBER USING SAME CAPACITANCE VALUE PERFORMS BETTER UNDER OVERLOAD

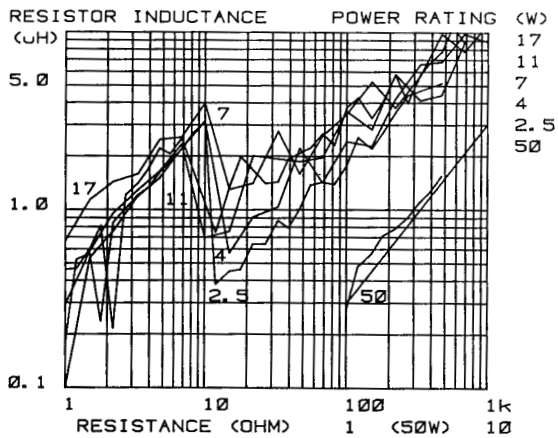

FIG.5 MEASURED PARASITIC INDUCTANCE OF CERAMIC-BODIED POWER WIREWOUND RESISTORS OF SEVERAL POWER RATINGS @ 10KHZ. UNSMOOTHED DATA ADEQUATE TO COVER TYPICAL VALUES AND TREND. RESULTS FOR METAL CLAD TYPES OFFSET.

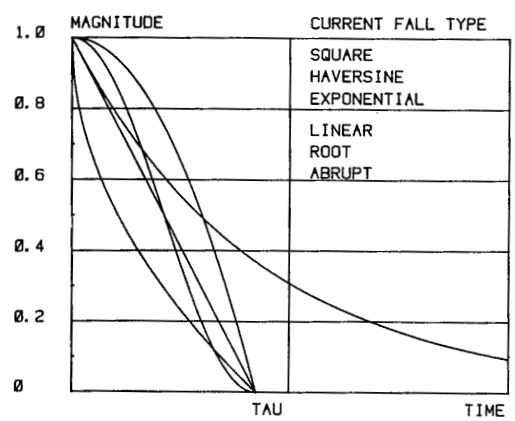

FIG.7 CURRENT-FALL SHAPES USED TO EXAMINE IMMUNITY OF RC-SNUBBERS TO SHAPE VARIATION. TAU EITHER DENOTES END OF FALL OR TIME-CONSTANT.

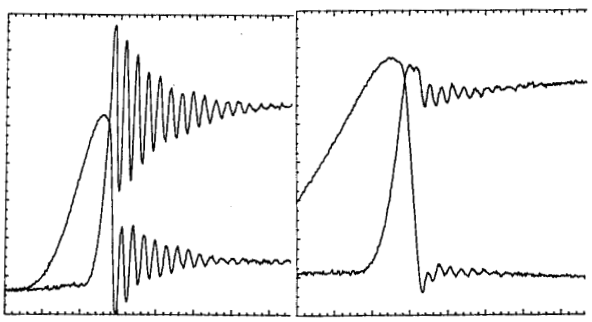

IGBT-MODULE DIODE
MG25H2YSYS1

Edc=550V
If=9A
di/dt=300A/µs
fo=44MHz

120V/div
6A/div
75ns/div

IGBT-MODULE DIODE
MG25H2YSYS1

Edc=550V
If=28A
di/dt=208A/µs

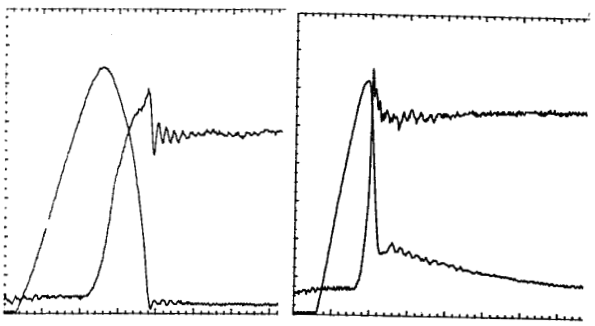

DISCRETE DIODE
BYT230-1000

Edc=550V
If=30A
di/dt=840A/µs

120V/div
10A/div
50ns/div

IGBT-MODULE DIODE
IXGQ25N100Y

Edc=550V
If=30A
di/dt=300A/µs

100V/div
5A/div
100ns/div

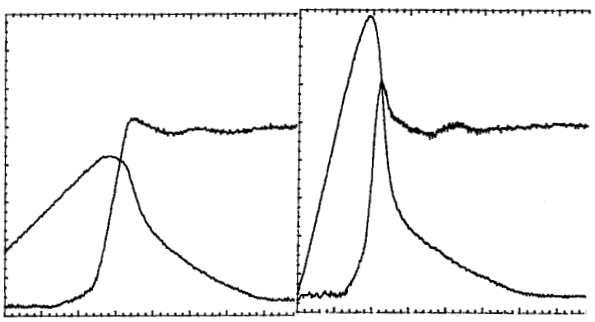

DISCRETE DIODE
SG35R120

Edc=600V
If=29A
di/dt=207A/µs

120V/div
10A/div
50ns/div

DISCRETE DIODE
SG35R120

Edc=600V
If=30A
di/dt=1090A/µs

120V/div
10A/div
50ns/div

FIG.6 DIODE REVERSE-RECOVERY WAVEFORMS FOR SEVERAL 30A DIODES UNDER DIFFERENT OPERATING CONDITIONS. VARIABILITY IN CURRENT-FALL SHAPE SHOWN.

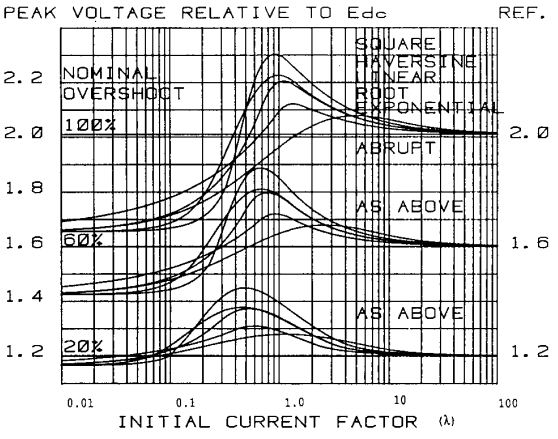

FIG.8 VARIATION IN OVERSHOOT ON SNUBBERS SET TO GIVE ABOUT 20,60 AND 100% OVERSHOOT. λ IS INVERSELY PROPORTIONAL TO CURRENT-FALL TIME.

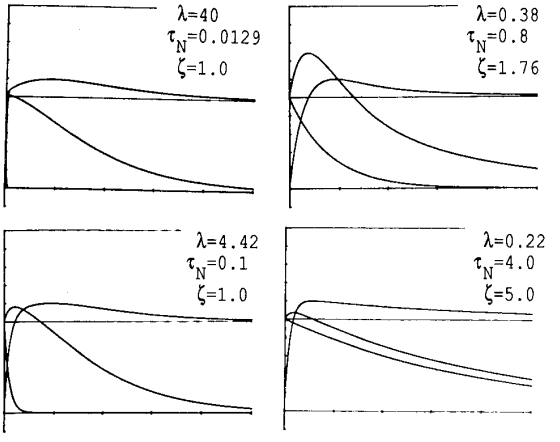

FIG.9 CALCULATED WAVEFORMS FOR λ, τ_N AND ζ VALUES GIVING 20% OVERSHOOT.

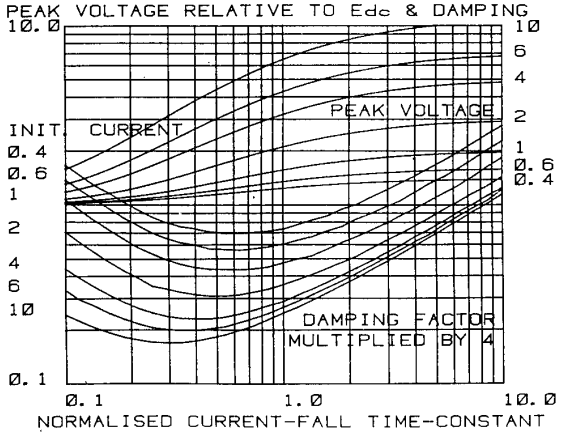

FIG.10 OVERSHOOT V_{OSN} AND DAMPING FACTOR, ζ, FOR OPTIMAL EXPONENTIAL SNUBBER FOR SEVERAL INITIAL CURRENT FACTORS, χ.

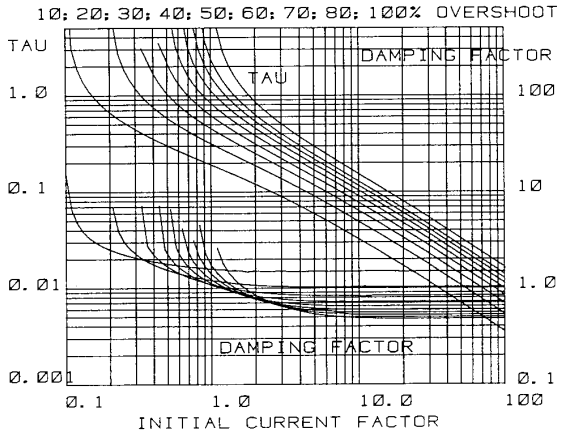

FIG.11 SET OF DESIGN CURVES FOR RC-SNUBBERS GIVING 10-100% OVERSHOOT WITH EXPONENTIAL CURRENT-FALL. TAU IS THE NORMALISED FALL TIME τ_N.

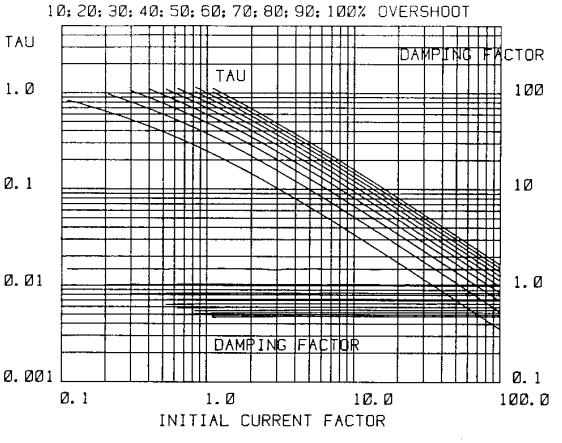

FIG.12 SET OF DESIGN CURVES FOR RC-SNUBBERS GIVING 10-100% OVERSHOOT WITH LINEAR DIODE CURRENT-FALL.

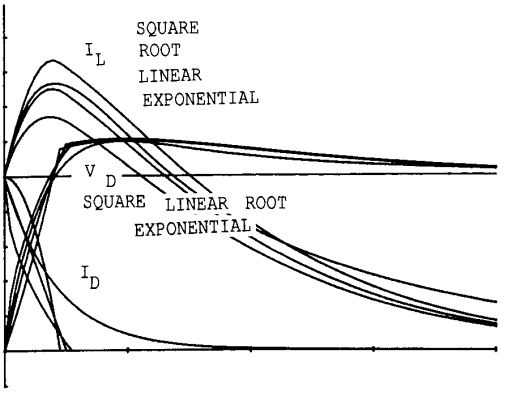

FIG.13a CALCULATED WAVEFORMS AT INTERSECTION POINTS OF 20% CURVES AND λ=0.7 LINE IN FIG.13.

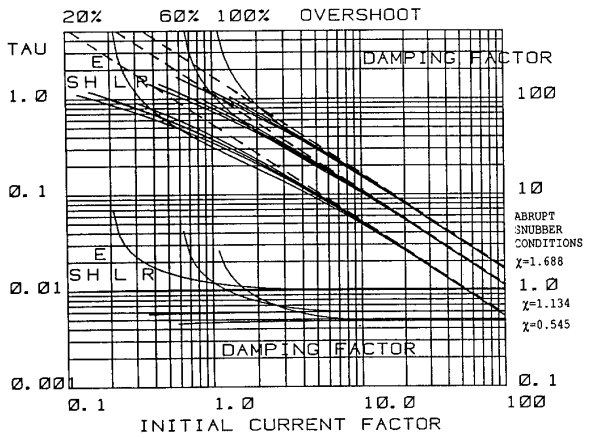

FIG.13 DESIGN CURVES AS FIG.11 BUT FOR ALL CURRENT-FALL TYPES.

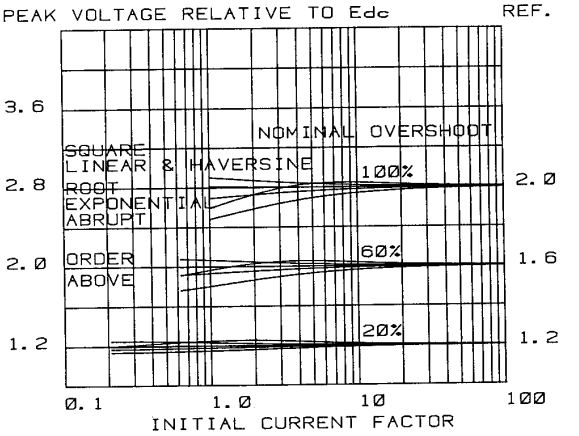

FIG.16 PEAK OVERSHOOT VARIATION ON 20,60 AND 100% LINEAR SNUBBERS WHEN USED WITH ALL CURRENT-FALL TYPES.

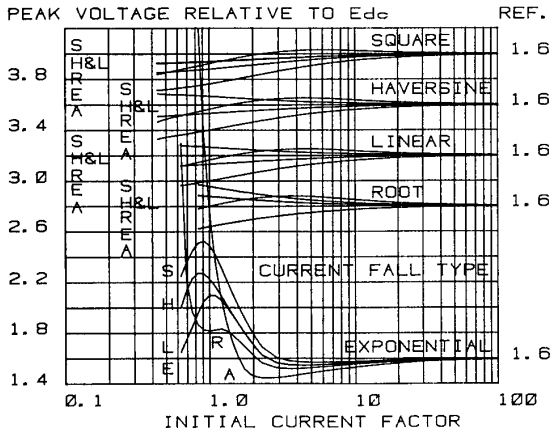

FIG.14 OVERSHOOT ON RC-SNUBBER SET TO GIVE 60% OVERSHOOT WITH LISTED CURRENT-FALL TYPE WHEN SUBJECTED TO ALL OTHER CURRENT-FALL SHAPES.

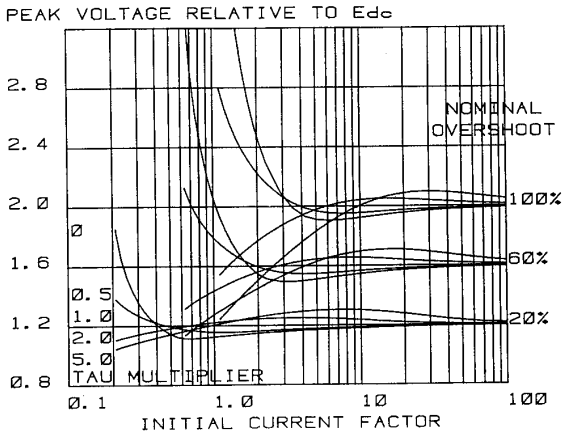

FIG.17 PEAK OVERSHOOT VARIATION ON 20,60 AND 100% EXPONENTIAL SNUBBERS WITH VARYING DIODE CURRENT-FALL DURATION.

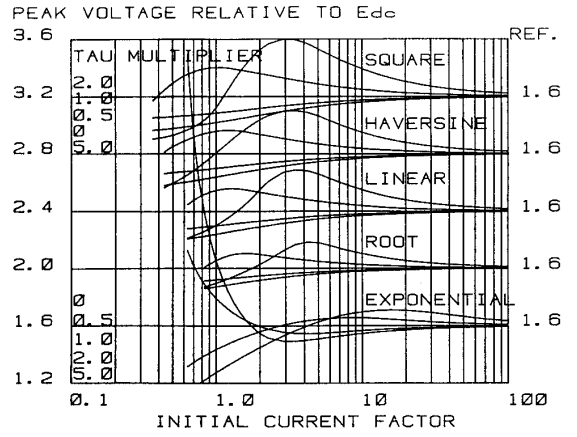

EXPONENTIAL SNUBBERS WITH VARYING DIODE CURRENT-FALL DURATION.

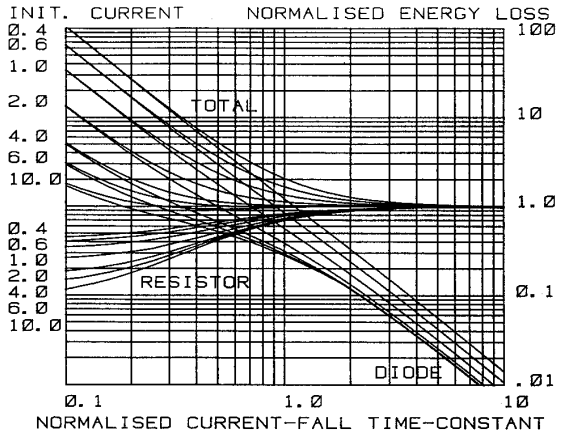

FIG.18 NORMALISED ENERGY-LOSS ASSOCIATED WITH EXPONENTIAL SNUBBERS. W_B (EQ.9b) NORMALISATION BASE.

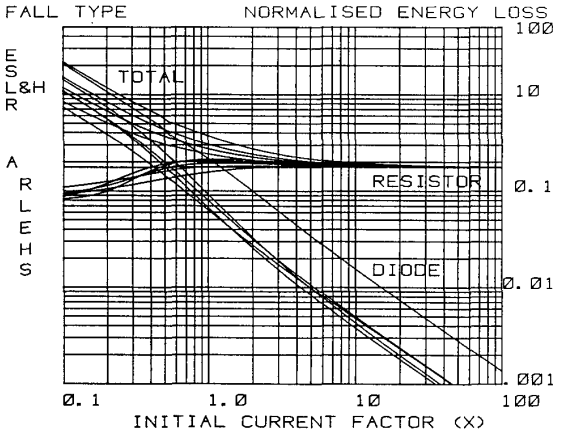

FIG.19 NORMALISED ENERGY-LOSS FOR SNUBBERS GIVING SPECIFIC OVERSHOOT LEVELS. W_B NORMALISATION BASE.

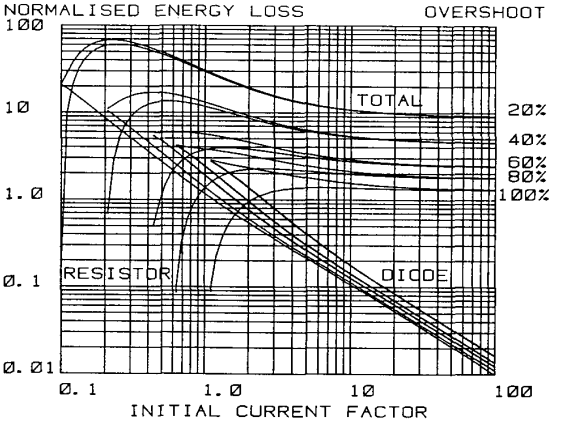

FIG.21 NORMALISATION ENERGY-LOSS FOR SNUBBERS GIVING SPECIFIC OVERSHOOT LEVELS . INITIAL TRAPPED ENERGY, $1/2L_S I_{RM}^2$, USED AS NORMALISATION BASE.

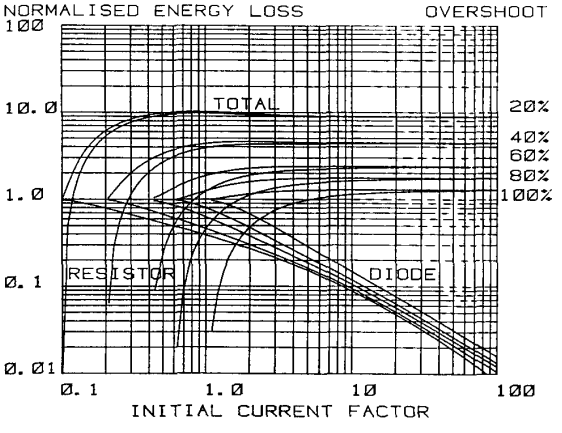

FIG.20 NORMALISED ENERGY-LOSS FOR SNUBBERS GIVING SPECIFIC OVERSHOOT LEVELS. W_B NORMALISATION BASE.

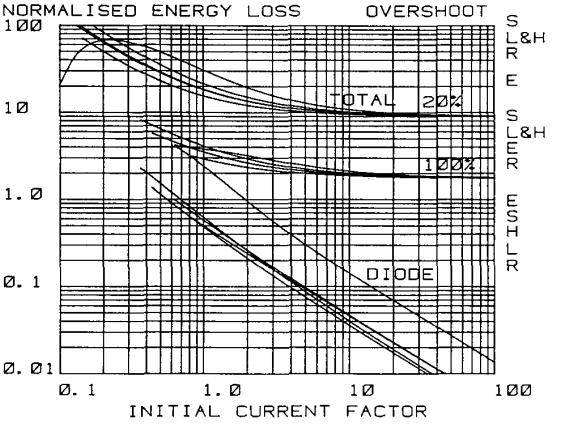

FIG.22 NORMALISED ENERGY-LOSS AS IN FIG.21 FOR ALL CURRENT-FALL TYPES.